Irradiation effects in InGaAs/InAlAs high electron mobility transistors

E. M. Jackson
SFA, Incorporated, 1401 McCormick Drive, Largo, Maryland 20875

B. D. Weaver[a)]
Naval Research Laboratory, Code 6818, Washington, DC 20375

S. Shojah-Ardalan and R. Wilkins
Prairie View A&M University, Prairie View, Texas 77446

A. C. Seabaugh
University of Notre Dame, Notre Dame, Indiana 46556

B. Brar
Rockwell Science Center, 1049 Camino Dos Rios, Thousand Oaks, California 91358

(Received 19 June 2001; accepted for publication 31 July 2001)

The radiation tolerance of high electron mobility transistors (HEMTs) based on InGaAs/InAlAs lattice matched to InP has been studied. At low fluences of 3 MeV He^{+} ions, the only effect is a reduction in the leakage currents. At higher fluences, the drain current decreases, the threshold voltage increases toward zero, and the transconductance decreases. These results are consistent with increased trapping in the donor layer and increased scattering in the channel layer. Radiation-induced increases in the threshold voltage occur three to nine times more slowly here than in GaAs/AlGaAs HEMTs, indicating high radiation tolerance. © *2001 American Institute of Physics.* [DOI: 10.1063/1.1408904]

Recently, InGaAs/InAlAs high electron mobility transistors (HEMTs) have shown great promise for electronic and optoelectronic applications. Transistor cut-off frequencies higher than 300 GHz have been achieved, and a number of circuits, including amplifiers, clock recovery circuits, and frequency dividers have been demonstrated.[1–4] However, before these devices can be used in spacecraft and other high-radiation environments, sufficient radiation tolerance must be achieved. Here, we report on radiation damage in HEMTs based on InGaAs/InAlAs lattice matched to InP.

The HEMT heterostructure consists of a modulation-doped InGaAs/InAlAs structure, with a two-dimensional electron gas (2DEG) above a superlattice buffer layer. The HEMTs are 50 μm in width, with a 0.25 μm gate length, and a source–drain spacing of 2.5 μm. The HEMTs have current gain cut-off frequencies f_T of 140 GHz and power gain cut-off frequencies $f_{\max}$ of 180 GHz. A more detailed description is given elsewhere.[5]

Samples were irradiated at room temperature with incremental fluences Φ of 3 MeV He^{+} ions at rates of about 3×10^{9} ions/cm^{2} s. Particles were incident 7° from the sample normal in order to prevent ion channeling effects. The range of the He^{+} ions in these materials is about 10 μm, so the damage (mostly point defects) is approximately uniform throughout the active region of the HEMTs. The source, drain, and gate of the HEMTs were grounded during irradiation.

dc electrical characteristics were measured using a Hewlett Packard HP4145B parameter analyzer with a HP Model 16056A test fixture. Data were taken before and after irradiation. All measurements were performed at room temperature.

With the source and substrate grounded, the drain current I_d was measured while the drain voltage V_d was swept from 0 to +2 V for fixed values of the gate voltage V_g between 0 and −1 V; thus producing a family of I_d–V_d curves. The transconductance ($G\equiv\delta I_d/\delta V_g$) was determined by measuring I_d as V_g was changed from 0 to −1.5 V in −0.075 V increments, and for $V_d=+0.5$, +1.25, and +2 V. Threshold voltages $V_{\rm th}$ were determined using the standard method of extrapolating from the point of maximum slope on the I_d–V_g curve along the asymptote to the zero-current intercept.

The dependence of I_d on V_g is shown in Fig. 1 for $V_d=0.5$ V. The general effects of irradiation are to decrease I_d

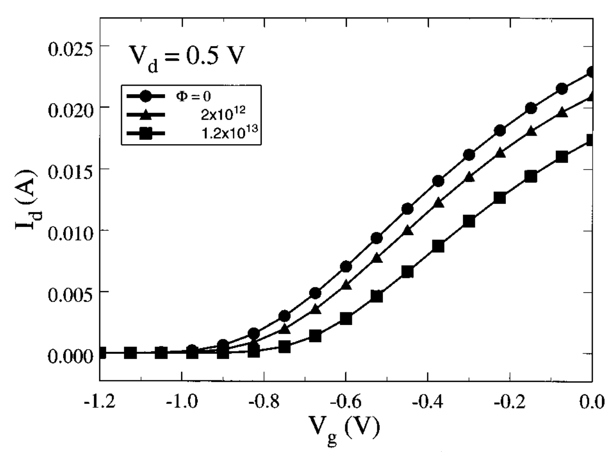

FIG. 1. Drain current vs gate voltage at $V_d=0.5$ V for several fluences of 3 MeV He^{+} ions is shown. At a fluence of 5×10^{10} cm^{-2}, the I_d–V_g curve is indistinguishable from the zero-fluence curve.

a)Electronic mail: weaver1@ccf.nrl.navy.mil

0003-6951/2001/79(14)/2279/3/$18.00

TABLE I. Threshold voltage and maximum transconductance at various fluences are shown.

Φ (He^+/cm^2)	G_m (mS)	V_{th} (V)
0	31 ± 1	-0.82 ± 0.02
$5\times10^{10}\pm20\%$	31	-0.82
$2\times10^{12}\pm10\%$	30	-0.78
$1.2\times10^{13}\pm10\%$	27	-0.70

uniformly across all V_g, increase V_{th} toward zero, and decrease the transconductance. Fluence-dependent values of V_{th} and the maximum transconductance G_m are given in Table I for $V_d=0.5$ V. Similar trends in I_d, V_{th}, and G have been observed in irradiated GaAs/AlGaAs and InGaAs/InGaP HEMTs.[6–8] The generally accepted explanation for radiation-induced decreases in G is a decrease in carrier density and mobility. Reduced mobility is caused by increased scattering of electrons from defects in the 2DEG, and decreased carrier density is due to scattering and charge trapping in the donor layer.

Radiation-induced increases in V_{th} have been reported previously for GaAs/AlGaAs HEMTs. However, the degree of radiation sensitivity is different in the InGaAs/InAlAs HEMTs studied here. In one set of GaAs/AlGaAs HEMTs, for example, a fluence of 5.5×10^{11}5 MeV He^{2+} ions/cm^{-2} caused V_{th} to increase by between 25 and 80 mV (i.e., 3%–8% of the initial value of V_{th}), depending on the device structure.[6] For the 3 MeV He^+ ions used here, an equivalent amount of displacement damage could be produced with a fluence of about 3.7×10^{11} He^+/cm^2. (The lower-energy ions create about 50% more damage per ion.) By interpolating between data points in Table I, we estimate that the corresponding change in V_{th} for the InGaAs/InAlAs HEMTs would be only 7 or 8 mV (0.9%–1.0% of the initial value of V_{th}), leading to a factor of about 3–9 times higher radiation tolerance in the threshold voltage of InGaAs/InAlAs HEMTs. The reason for the greater tolerance is currently not known.

Curves of I_d versus V_g are shown in Fig. 2 for $V_d=2$ V. The same general trends can be seen as for $V_d=0.5$ V, but at $V_d=2$ V, the I_d–V_g curves change shape as the fluence is increased. The "knees" that appear in the data for $\Phi>0$ correlate with peaks and valleys in the transconductance curves, as shown in the inset of Fig. 2. Data were also taken at $\Phi=5\times10^{10}$ He^+/cm^2, but are not shown in Figs. 1–3 because no radiation-induced changes in I_d, V_{th}, or G were observed.

Curves of I_d versus V_d are shown in Fig. 3 for various V_g and Φ. Three effects of irradiation are evident. First, as in Figs. 1 and 2, the drain current decreases with irradiation. Second, kinks appear and third, a region of negative differential resistance (NDR) occurs at the highest fluence for drain voltages between 1 and 1.5 V, and for $V_g>-0.5$ V. Features such as kinks have been studied extensively in unirradiated HEMTs, and are generally attributed either to electron trapping in the donor layer or impact ionization.[9,10] The appearance of NDR generally implies the onset of real-space charge transfer, wherein electrons are dynamically shunted from the 2DEG in the channel into the InAlAs barrier layer.[11–13] Kinks and NDR do not occur at lower drain voltages, such as in Fig. 1.

The gate leakage current I_g is plotted in Fig. 4 against V_g for various Φ, and for $V_d=1.25$ V. Similar data are shown in the inset of Fig. 4 for $V_d=0.5$ V. For the unirradiated device, I_g tends to zero as V_g approaches zero, with the exception of the hump in I_g between $V_g=-1.25$ V and -0.6

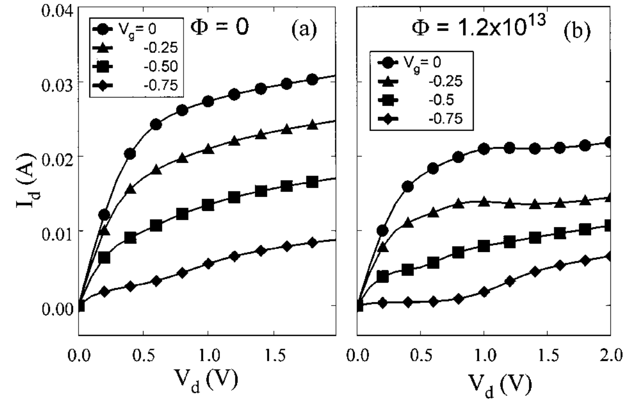

FIG. 3. (a) Drain current vs drain voltage for several gate voltages before irradiation is shown. (b) Drain current vs drain voltage for several gate voltages after irradiation to a fluence of 1.2×10^{13} cm^{-2} 3 MeV He^+/cm^2 is presented.

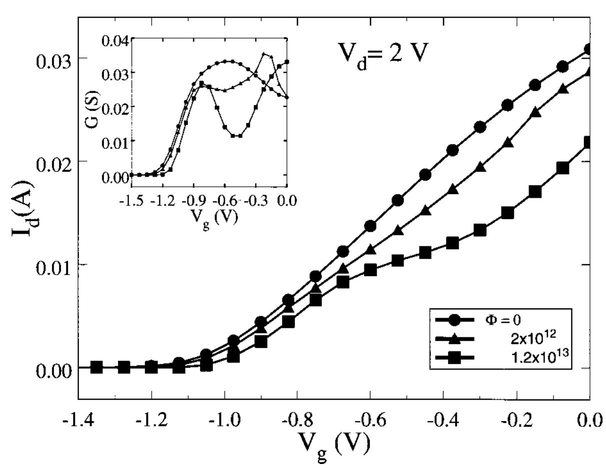

FIG. 2. Drain current vs gate voltage at $V_d=2.0$ V for several fluences of 3 MeV He^+ ions is shown. Inset displays corresponding transconductance curves.

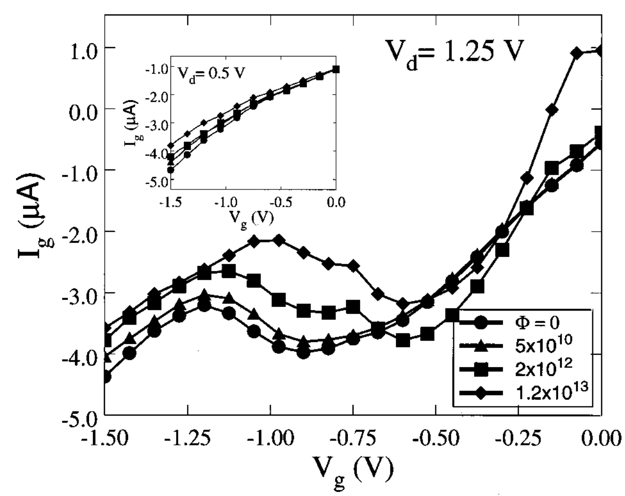

FIG. 4. Gate leakage current vs gate voltage at several fluences and for $V_d=1.25$ V is shown. Inset displays similar curves at $V_d=0.5$ V.

V, and for $V_d = 1.25$ V. Radiation damage generally reduces the magnitude of I_g toward zero.[14]

One notable variation on the radiation-induced decrease of $|I_g|$ occurs at the highest fluence, and for small gate voltages ($V_g < V_d, V_s$). In that instance, $|I_g|$ not only decreases toward zero, but changes sign and becomes positive.

Enhanced carrier removal by trapping, enhanced scattering of carriers out of the 2DEG, and possibly an increased series resistance explain all the trends observed here except the NDR, and the change in sign in I_g—both of which occur only at large V_d.

We propose the following scenario. When V_d is large, electrons in the channel have enough kinetic energy to overcome the barrier into the InAlAs, but before irradiation their momentum is directed perpendicular to the barrier. Radiation damage causes scattering and/or heating which shunts some electrons into the InAlAs.[15] The NDR and the kinks occur because electron mobility is lower in the InAlAs than in the InGaAs channel.[16] Some of the electrons scattered into the barrier layer have enough energy to reach the gate despite the negative value of V_g. As the gate voltage approaches zero, the energy required for an electron to reach the gate decreases, and the number of electrons transferred into the InAlAs increases until the electron current exceeds the negative gate current components, and I_g changes sign.

We conclude that, as in most other field-effect devices, the main effects of displacement damage in InGaAs/InAlAs HEMTs are carrier removal by trapping and carrier mobility decrease by scattering from radiation-induced defects in the 2DEG.[17] These two effects, in addition to a possible increase in series resistance and several interesting dynamic effects at larger drain voltages and damage levels, describe the radiation response of the HEMTs quite well. In addition, we find that it might be possible to use radiation to reduce leakage currents in InGaAs/InAlAs HEMTs without otherwise degrading device performance. Finally, due to their high radiation tolerance, InGaAs/InAlAs HEMTs on InP have good prospects for application in radiation environments.

This work was supported in part by the Office of Naval Research, and by NASA under Contract Nos. NCC 9-50 and NCC 9-114.

[1] Y. Yamashita, A. Endoh, M. Higashiwaka, K. Hikosaka, T. Mimura, S. Hayamizu, and T. Matsui, Jpn. J. Appl. Phys., Part 2 **39**, L838 (2000).
[2] Y. Umeda, K. Osafune, T. Enoki, H. Yokohama, and Y. Ishii, IEEE Trans. Electron. **82**, 1080 (1999).
[3] K. Murata and Y. Yamane, Electron. Lett. **36**, 1617 (2000).
[4] C. Pobanz, M. Matloubian, V. Radisic, G. Raghavan, M. Case, M. Micovic, M. Hu, C. Nguyen, S. Weinreb, and L. Samoska, *2000 Int. Conf. InP and Related Mat.* (IEEE, Piscataway, NJ, 2000), p. 67.
[5] A. Seabaugh, B. Brar, T. Broekaert, F. Morris, P. Van der Wagt, and G. Frazier, Solid-State Electron. **43**, 1355 (1999).
[6] G. J. Papaioannou, M. J. Papastamatiou, and A. Christou, J. Appl. Phys. **78**, 3066 (1995).
[7] H. Ohyama, E. Simeon, S. Kuroda, C. Claeys, Y. Takami, T. Hakata, K. Kobayashi, M. Nakabayashi, and H. Sunaga, Microelectron. Reliab. **41**, 79 (2001).
[8] H. Ohyama, E. Simeon, S. Kuroda, C. Claeys, Y. Takami, T. Hakata, and H. Sunaga, IEEE Trans. Nucl. Sci. **45**, 2861 (1998).
[9] B. Georgescu, M. A. Py, A. Souffi, G. Post, and G. Guillot, Electron. Lett. **19**, 154 (1998).
[10] M. H. Somerville, K. A. del Alamo, and W. Hoke, Electron. Lett. **17**, 473 (1996).
[11] S. R. Bahl, W. J. Azzam, and J. A. del Alamo, IEEE Trans. Electron Devices **38**, 1986 (1991).
[12] *Modern Semiconductor Physics*, edited by S. M. Sze (Wiley, New York, 1998), p. 298.
[13] S. R. Bahl, W. J. Azzam, and J. A. del Alamo, IEEE Trans. Electron Devices **38**, 1986 (1991).
[14] R. Wilkins, S. Shojah-Ardalan, W. P. Kirk, G. F. Spencer, R. T. Bate, A. C. Seabaugh, R. Lake, P. Stelmaszyk, A. D. Wieck, and T. N. Fogarty, IEEE Trans. Nucl. Sci. **46**, 1702 (1999).
[15] D. Widiger, I. C. Kizilyalli, K. Hess, and J. J. Coleman, Superlattices Microstruct. **1**, 465 (1985).
[16] S. R. Bahl, W. J. Azzam, and J. A. del Alamo, IEEE Trans. Electron Devices **38**, 1986 (1991).
[17] *Handbook of Radiation Effects*, edited by A. Holmes-Siedle and L. Adams (Oxford University Press, Oxford, 1993), p. 84.